

Suspended Sediment Fluxes in a Tidal Wetland: Measurement, Controlling Factors, and Error Analysis

NEIL K. GANJU*, DAVID H. SCHOELLHAMER, and BRIAN A. BERGAMASCHI

U.S. Geological Survey, Placer Hall, 6000 J Street, Sacramento, California 95819

ABSTRACT: Suspended sediment fluxes to and from tidal wetlands are of increasing concern because of habitat restoration efforts, wetland sustainability as sea level rises, and potential contaminant accumulation. We measured water and sediment fluxes through two channels on Browns Island, at the landward end of San Francisco Bay, United States, to determine the factors that control sediment fluxes on and off the island. In situ instrumentation was deployed between October 10 and November 13, 2003. Acoustic Doppler current profilers and the index velocity method were employed to calculate water fluxes. Suspended sediment concentrations (SSC) were determined with optical sensors and cross-sectional water sampling. All procedures were analyzed for their contribution to total error in the flux measurement. The inability to close the water balance and determination of constituent concentration were identified as the main sources of error; total error was 27% for net sediment flux. The water budget for the island was computed with an unaccounted input of $0.20 \text{ m}^3 \text{ s}^{-1}$ (22% of mean inflow), after considering channel flow, change in water storage, evapotranspiration, and precipitation. The net imbalance may be a combination of groundwater seepage, overland flow, and flow through minor channels. Change of island water storage, caused by local variations in water surface elevation, dominated the tidally averaged water flux. These variations were mainly caused by wind and barometric pressure change, which alter regional water levels throughout the Sacramento-San Joaquin River Delta. Peak instantaneous ebb flow was 35% greater than peak flood flow, indicating an ebb-dominant system, though dominance varied with the spring-neap cycle. SSC were controlled by wind-wave resuspension adjacent to the island and local tidal currents that mobilized sediment from the channel bed. During neap tides sediment was imported onto the island but during spring tides sediment was exported because the main channel became ebb dominant. Over the 34-d monitoring period 14,000 kg of suspended sediment were imported through the two channels. The water imbalance may affect the sediment balance if the unmeasured water transport pathways are capable of transporting large amounts of sediment. We estimate a maximum of 2,800 kg of sediment may have been exported through unmeasured pathways, giving a minimum net import of 11,200 kg. Sediment flux measurements provide insight on tidal to fortnightly marsh sedimentation processes, especially in complex systems where sedimentation is spatially and temporally variable.

Introduction

Tidal marshes are depositional environments characterized by emergent vegetation, fine sediment substrates, and dendritic channel networks. They are common in deltaic settings and in sheltered coastal areas where fine sediments accumulate to a level where wetland plants can colonize. Several factors are credited with maintaining the presence of these wetlands, such as accumulation due to autochthonous detritus and deposition due to storms (Goodbred and Hine 1995; Nyman et al. 1995), wind-generated high water levels (Bartholdy et al. 2004), river flooding (Cahoon et al. 1996), and regular tidal inundation via tidal creeks (Leonard 1997). Recent interest in tidal marshes springs from their role in the ecological framework as habitats for valued flora and fauna. Due to the biological value of these systems, many regulatory agencies seek to restore lost tidal marshes and protect existing areas from drainage or development.

Ecological concerns regarding habitat and contaminants highlight the need for understanding marsh accretion processes. The import-export of suspended sediment plays a large role in the formation and maintenance of tidal wetlands, as well as in the overall sediment budget within an ecosystem (Cahoon et al. 1996; Yang 1998). A decrease in sediment supply can halt the accretion necessary for wetland survival. In consideration of the ongoing rise in sea level, fluxes of material to and from tidal marshes may control their sustainability (Pont et al. 2002; Temmerman et al. 2004) and must be quantified. The presence of sediment-associated contaminants increases the relevance of marsh accretion, especially for studies of contaminant uptake and transformation within wetlands (e.g., Marvin-DiPasquale and Agee 2003).

Ultimately the quantification of sediment fluxes will assist in relevant management decisions. Previous work has established the variability of fluxes within tidal creek cross sections (Pillay et al. 1992), as well as the need for continuous, long-term data (Suk et al. 1999). In this study we measure water and sediment flux at an established tidal wetland,

*Corresponding author; tele: 916/278-3117; fax: 916/278-3013; e-mail: nganju@usgs.gov

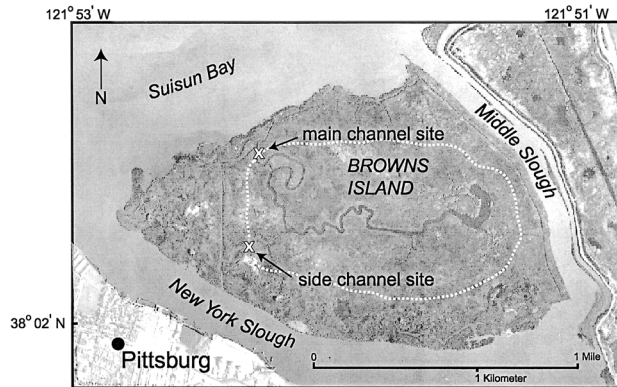


Fig. 1. Inset map of Browns Island. Main and side channel sites shown, as well as assumed drainage area of channels (dashed line).

providing insight on the processes that determine net flux. Due to the tidal variability of these parameters, continuous data must be collected to gain reasonable flux estimates. Cross-sectional variability also must be considered.

An established wetland was chosen to serve as a model for estimating mature marsh fluxes, representing the end point of restoration efforts, as well as natural marsh conditions. Browns Island (Fig. 1) is a *Scirpus* (tule) marsh located at the confluence of the Sacramento-San Joaquin River Delta and Suisun Bay, California (Fig. 1). This wetland was chosen based on accessibility, age, and measurement feasibility. Sea-level rise and decreasing sediment supply from the watershed (Wright and Schoellhamer 2004) threaten future sustainability of established and restored wetlands in the Delta and Suisun Bay.

Measurement Methods

SITE DESCRIPTION

Browns Island features a main drainage channel (Fig. 1) that runs from a lagoon located in the interior of the island to Suisun Bay, while a side channel runs from the main channel to New York Slough. The main channel is approximately 17 m wide with a maximum depth of 4.5 m at high water, while the side channel has a width of 13 m and a maximum depth of 3.7 m (Figs. 1 and 2). At low tide, the steep vertical edges of the vegetated marsh are visible, with mudflats exposed on the channel edges. Numerous side channels exist near the mouth, so the main channel measurement site was chosen upstream of these channels, 300 m from the mouth. The side channel site was chosen based on vegetative cover and accessibility, about 400 m from New York Slough. Deployment began October 10, 2003, and instruments were retrieved November 13,

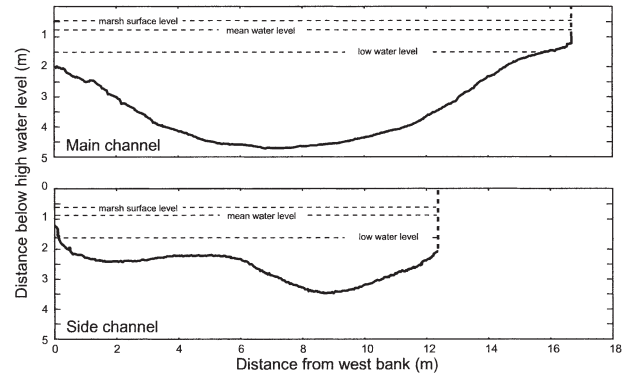


Fig. 2. Geometry of main channel and side channel. Geometries were determined by acoustic Doppler data from discharge measurements.

2003. This period coincided with the transition between dry and wet seasons. Regional suspended sediment concentrations (SSC) are typically at a minimum during this season (Krone 1979).

Mixed semidiurnal tidal forcing causes a maximum spring tidal range of 1.8 m and a minimum neap tide range of 0.20 m at Pittsburg, California (Fig. 1). Freshwater outflow from the Delta (and past Browns Island) is regulated by the California Department of Water Resources (2002), with the majority of flow occurring during the wet season (December–May) due to rainfall, snowmelt, and reservoir releases. Flow is regulated during the dry season to keep the 2 psu salinity limit seaward of the Delta.

DISCHARGE

The index velocity method (Simpson and Bland 2000) provides a procedure to measure discharge continuously with surrogate measurements. The continuous velocity measured by an upward-looking acoustic Doppler velocity meter (ADVM), known as the index velocity (V_i), is calibrated to instantaneous measurements of channel-average velocity (V_{ca}), as measured by a downward-looking acoustic Doppler current profiler (ADCP). The continuous depth (h) measured by the ADVM also is calibrated to instantaneous channel area measurements (A), yielding a stage-area relationship. The product of A and V_{ca} is discharge (Q). Total flux then is the product of constituent concentration and discharge. This procedure was applied in both the main and side channels.

An upward-looking ADVM (Sontek Argonaut 3-MHz XR, San Diego, California) was deployed on the bed. The ADVM was programmed to collect the depth-averaged velocity above the unit for 6 min during the beginning of every 15-min period. These data are the V_i . In addition to collecting V_i data, the unit also collects depth measurements.

During strong spring tides, a downward-looking ADCP (RD Instruments 1.2-MHz Workhorse, San Diego, California) mounted on a small (1 m length) tethered boat was repeatedly towed across the channel to obtain instantaneous discharge measurements through one tidal cycle. Channel area was measured using the geometry of the channel cross section (provided by the ADCP) and the appropriate water-surface elevation. By dividing the instantaneous discharge by the corresponding instantaneous channel area, instantaneous V_{ca} is obtained. Linear regression is used to relate the V_i readings with the corresponding instantaneous V_{ca} measurements. This yields a calibration curve that is applied to create a continuous time series of V_{ca} .

The time series of channel area is constructed using the channel geometry and the water-surface elevation record. The relation between depth and channel area is applied to the depth time series collected by the ADVM to yield a continuous time series of channel area. The continuous time series of V_{ca} is multiplied by the continuous time series of channel area to yield a continuous time series of discharge through the channel. A low-pass Butterworth filter with a cutoff frequency of $1/30 \text{ h}^{-1}$ was applied to yield the tidally averaged discharge, which assists in evaluating the frequency of forcing mechanisms.

METEOROLOGICAL DATA

Meteorological forcings are known to modulate hydrodynamic processes in estuaries, so atmospheric data from Met and Twitchell Islands (2 and 10 km to the west and east of Browns Island, respectively) were collected to assist in data interpretation. Parameters measured at site Met include wind speed, wind direction, and barometric pressure, while precipitation and evapotranspiration data are collected at site TWI. Data from site TWI were obtained from the California Irrigation Management Information System (www.cimis.water.ca.gov). Wind speed was decomposed into east-west components and filtered in the same manner as mentioned above, as was the change in barometric pressure.

SUSPENDED SEDIMENT CONCENTRATIONS

A Hydrolab DS4a instrument (Hydrolab, Austin, Texas), equipped with sensors for specific conductance, temperature, depth, pH, and turbidity, was deployed on a frame on the channel bed. The instrument was recovered weekly for cleaning and data retrieval, as well as calibration checks with known standards. The nephelometric turbidity sensor reports in nephelometric turbidity units (NTU). Because optical characteristics of sediment vary with particle size and composition, water

samples must be collected to calibrate the sensor for local sediment characteristics. Water samples were collected to relate NTU to SSC, in milligrams per liter of suspended sediment.

WATER SAMPLING

Water samples were collected using an isokinetic D-77 bottle sampler with a 0.25 in-diameter nozzle (Edwards and Glysson 1999). To accurately represent the average conditions in the channel, equal-discharge-increment (EDI) sampling was desired. By collecting depth-integrated samples at discharge centroids, the EDI method approximates the channel-average conditions. Knowledge of the flow distribution in the channel allows for the collection of these samples. Several ADCP measurements were made to determine the flow distribution and to locate five discharge centroids. Analysis of the flow measurements indicated that using five equally spaced centroids was satisfactory. The sampler, connected by cable and reel to the vessel, is lowered to just above the bed and raised to the surface at an appropriate transit rate such that an equal water volume is collected in the bottle at each centroid location. This provides a vertically integrated sample at five points across the section. This procedure was performed for the main channel only; side channel point samples were collected with a Van Dorn sampler due to reduced channel size.

Sensor output (NTU) from the median time of the sample was related to the actual channel-average SSC providing a calibration curve. Applying the calibration curve to the continuous sensor record provides a continuous record of channel-average SSC.

FLUX CALCULATION

The decomposition of the total constituent flux is given by Fischer et al. (1979). Lateral and vertical variations of SSC can be ignored in the main channel because depth-integrated, discharge-weighted water samples were collected, while these variations are not considered major in the smaller side channel. The flux decomposition reduces to:

$$\begin{aligned}
 [F] = & [u][A][c] + [u'[A][c]] + [[u]A'[c]] + [u'A'[c]] \\
 & (1) \qquad (2) \qquad (3) \qquad (4) \\
 & + [[u][A]c'] + [u'[A]c'] + [[u]A'c'] + [u'A'c'] \\
 & (5) \qquad (6) \qquad (7) \qquad (8)
 \end{aligned}$$

where $[F]$ is the total discharge-weighted residual flux, u is the V_{ca} , A is the channel area, and c is the constituent concentration (SSC). Brackets denote a tidally averaged value, while the prime indicates the deviation of the instantaneous value from the

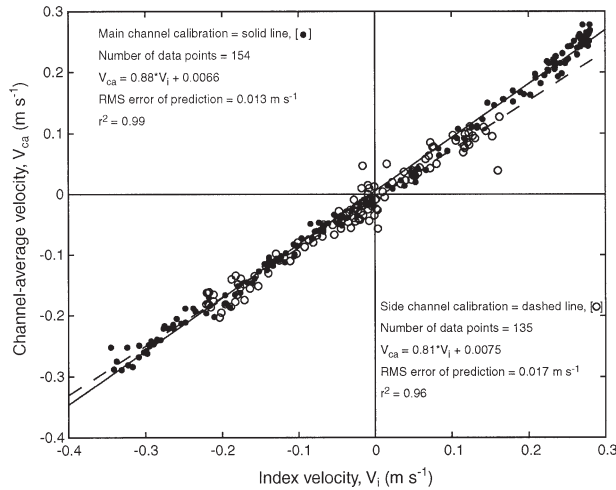


Fig. 3. Calibration of index velocity (V_i) to channel-average velocity (V_{ca}) from main and side channels. Positive values indicate flood direction (towards island interior), negative values indicate ebb direction (towards Suisun Bay).

tidally averaged value, i.e., $c' = c - [c]$. Tidal averaging was performed using a low-pass Butterworth filter with a cutoff frequency of $1/30 \text{ h}^{-1}$. The filter was applied in the forward and reverse directions to minimize anomalies at the end points of the record.

The advective and dispersive flux terms (terms 1 and 6) dominate total flux, while Stokes drift (term 4) contributes a minor portion. The remaining terms usually are negligible. Flux components from the main and side channel were summed to yield flux time series for the island as a whole.

Results and Discussion

DISCHARGE

V_i measurements were collected successfully every 15 min between October 10 and November 13, 2003. V_{ca} measurements were made in both channels, approximately every 3 min for 12 h during a spring tidal cycle. The V_i record was interpolated onto the V_{ca} record, using the median time of each respective measurement. A calibration curve was developed for V_{ca} as a function of V_i , separately for each channel (Fig. 3). The good fits indicate suitable site selection in each channel.

Depths were successfully measured in each channel on a continuous basis by the upward-looking ADVMs. The channel profiles were measured using the tethered, boat-mounted, downward-looking ADCP, when the water level was at marsh surface. Area at 0.3-m intervals of depth was determined and a quadratic fit was applied (Fig. 4). Vertical channel walls were assumed above marsh level, due to negligible flow within *Scirpus* marsh canopies at higher tides (Yang 1998).

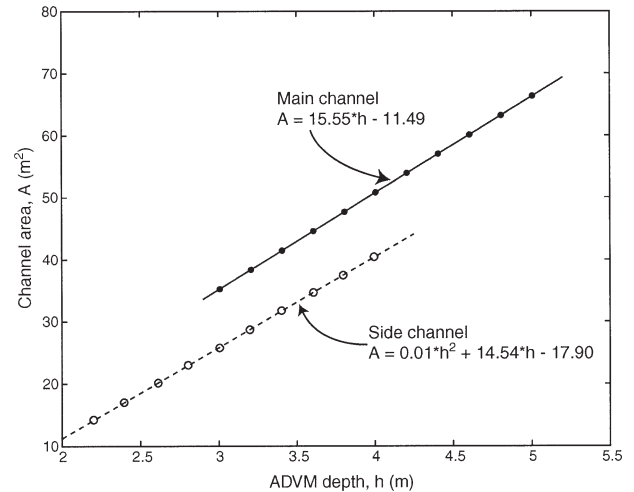


Fig. 4. Calibration of acoustic Doppler velocity meter (ADVM) depth (h) to channel area (A) from main and side channels.

The calibrated, continuous time series of V_{ca} and channel area were multiplied to yield a continuous time series of main and side channel discharge, which was summed to yield total discharge (Fig. 5). The instantaneous time series demonstrates a significant ebb dominance during spring tides, though the net filtered (tidally averaged) discharge is close to zero. Peak instantaneous ebb flow is 35% greater than flood flow. This dominance disappears during neap tides, when maximum flood and ebb flows are similar. The net water discharge for the main channel is landward (flood-biased), while net discharge is seaward (ebb-biased) in the side channel. This implies that some portion of water

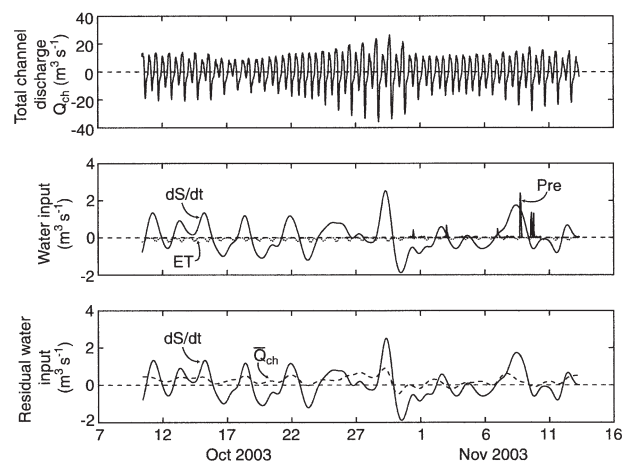


Fig. 5. Total channel discharge (sum of main and side channel discharges); measured evapotranspiration (ET), precipitation (Pre), and estimated storage change (dS/dt); and comparison of filtered discharge (\bar{Q}_{ch}) and change in storage. Positive values indicate input, negative values indicate output.

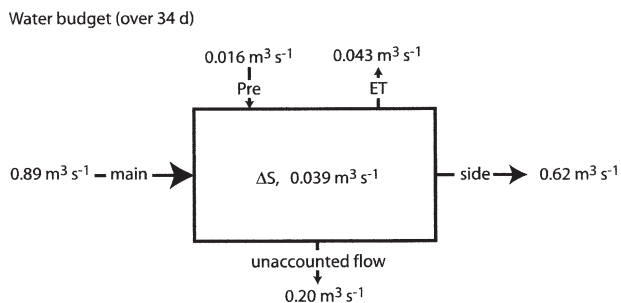


Fig. 6. Water budget for Browns Island. Mean instantaneous values over monitoring period are given. Pre is precipitation, ET is evapotranspiration, ΔS is change in storage.

entering the main channel on flood is diverted through the side channel on ebb.

Estimation of evapotranspiration, precipitation, and storage change were performed to close the water balance (Fig. 5). The vertical and horizontal water flux through tidal wetlands has been investigated by several authors; tidal inundation is found to affect expansion, compression, and storage within the island (e.g., Hemond and Fifield 1982; Nuttle 1988). Due to the possible heterogeneity, expansion, and contraction of the peat matrix, porosity was assumed to be equal to 1. Drainage area (1.3 km^2) was conservatively estimated as half the total surface area of the island by inspection of aerial photographs (Fig. 1). The change in tidally averaged water level (at the main channel site) was multiplied by an estimate of the drainage area (and accompanying porosity) to yield the volume of water stored in the island. Precipitation and evapotranspiration time series were also multiplied by the drainage area to convert water levels to water volumes.

Once the inputs (flood tide flow, precipitation), outputs (ebb tide flow, evapotranspiration), and storage changes (change in island water storage) are considered, the mean water imbalance averaged over the entire deployment is reduced to $0.20 \text{ m}^3 \text{ s}^{-1}$, which is 22% of the mean measured instantaneous inflow (Fig. 6). This imbalance is the flux of water that enters the island and is not accounted for in outflow. Groundwater seepage in peat marshes has been conservatively estimated at 5.0 mm d^{-1} (Hemond et al. 1984). This infiltration rate, when multiplied by the estimated drainage area, is $0.08 \text{ m}^3 \text{ s}^{-1}$. The remaining net input, $0.12 \text{ m}^3 \text{ s}^{-1}$, could easily be exported by a combination of multiple unmeasurable creeks and overland flow. Measurement error may also be introduced by variable index velocity and stage area rating curves; environmental conditions may vary during periods when calibration data were not collected.

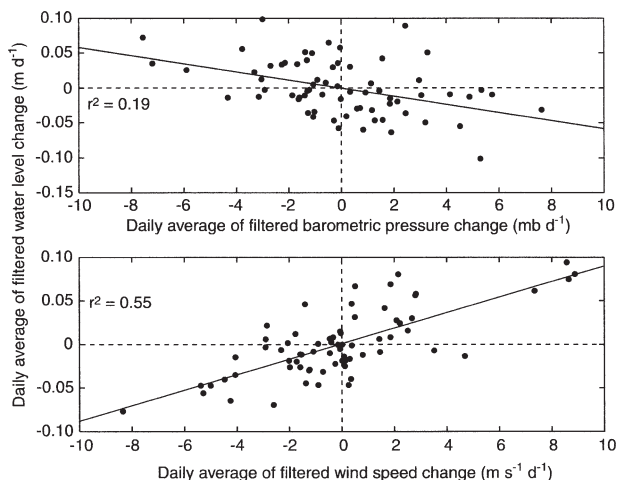


Fig. 7. Regression of filtered water level change against filtered barometric pressure change and filtered wind speed change.

METEOROLOGICAL FORCING

Water storage changes within Browns Island dominate the residual water flux as compared to the residual water flux through the channels alone (Fig. 5). These changes are attributed primarily to wind and barometric pressure changes on a regional scale, which influence local water levels (Fig. 7). Increasing westerly winds tend to increase water surface elevations in the eastern portions of the bay and storage in Browns Island, while relaxing winds reverse this effect. Increasing barometric pressure tends to decrease water levels and storage in Browns Island and the estuary as a whole (Walters and Gartner 1985). This has the effect of increasing seaward flow, while decreasing pressure increases storage and decreases seaward flow (Tobin et al. 1995).

CONTINUOUS TIME SERIES OF SUSPENDED SEDIMENT CONCENTRATIONS

The optical sensors successfully collected data in both channels between October 10 and November 13, 2003. The raw sensor output was edited to remove spikes and anomalies in the record, usually caused by debris. The optical sensor output calibrations (Fig. 8) were applied to the respective time series of sensor output, to yield a continuous time series of channel-average SSC in both channels (Fig. 9). At SSC below 10 mg l^{-1} the main channel instrument response was zero, resulting in clipping below this level.

Tidal velocities and wind are the major mechanisms for sediment transport to and from Browns Island. Resuspension of bottom sediment in the main channel by relatively large ebb velocities causes peaks in SSC to correspond with velocity

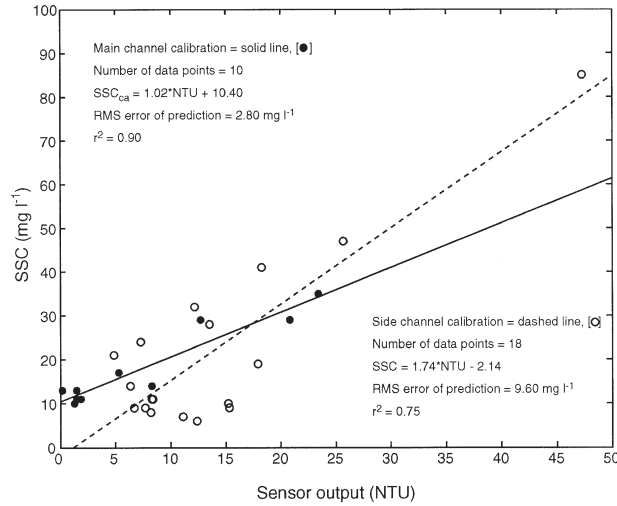


Fig. 8. Calibration of nephelometric turbidity units (NTU) to channel-average suspended sediment concentrations (SSC) for both main and side channels.

peaks (Fig. 10). Because the side channel is an ebb-biased outlet for the main channel, SSC maxima during ebb in the main channel are advected through the side channel. The separation between peaks is due to the distance between the sites; peak SSC in the side channel coincides with the end of ebb tide, indicating that advection is the mechanism for increased SSC. Flood tide SSC is dependent on SSC in Suisun Bay (for the main channel) and possibly New York Slough (for the side channel). Wind events contribute to increased SSC in Suisun Bay via wind-wave resuspension (Ruhl and Schoellhamer 2004); those resuspended sediments are

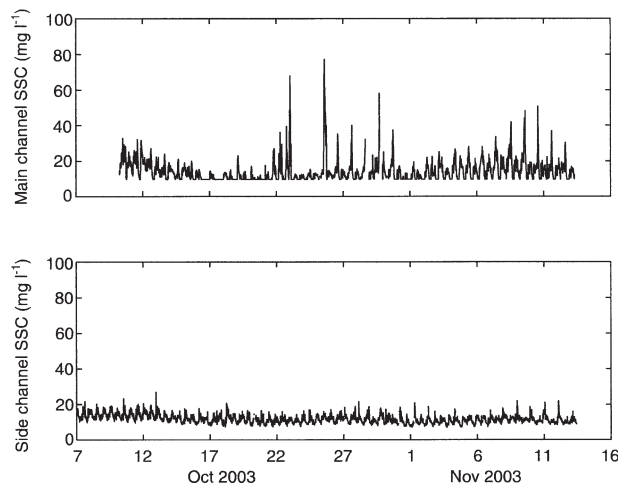


Fig. 9. Continuous time series of channel-average suspended sediment concentrations (SSC) for main channel and side channel. Poor resolution in low SSC range resulted in clipping below 10 mg l^{-1} in main channel.

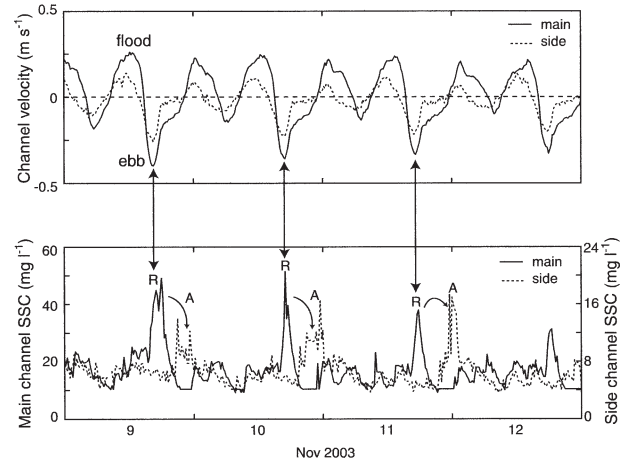


Fig. 10. Subset of main channel velocity (flood tide = positive) and main and side channel suspended sediment concentrations (SSC). Resuspension peaks (R) in main channel are complemented by advection peaks (A) in side channel on ebb tide.

imported to Browns Island on flood tide, leading to a correlation between filtered change in wind speed and SSC (Fig. 11). The large shoal outside the mouth of Browns Island is susceptible to wind-wave resuspension as well. This study coincided with minimal freshwater flow from the Delta; during elevated freshwater flow it can be expected that regional SSC would increase (Krone 1979), increasing flood-tide SSC within Browns Island.

SUSPENDED SEDIMENT FLUX CALCULATION

Advective flux, Stokes drift flux, and dispersive flux (terms 1, 4, and 6, respectively) accounted for

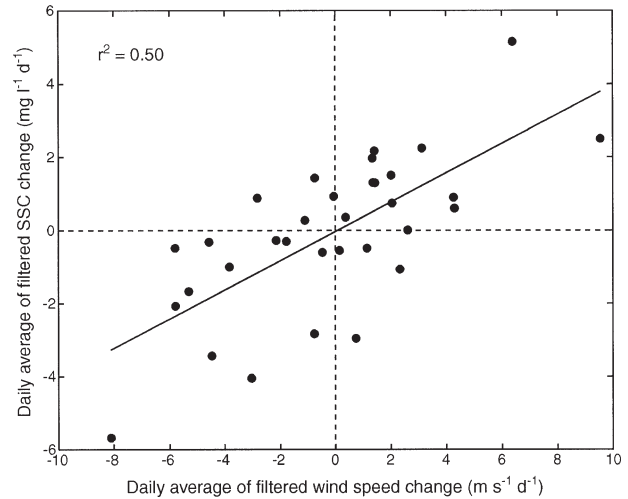


Fig. 11. Regression between filtered suspended sediment concentration (SSC) change and filtered wind speed change. Increasing winds increase wind-wave resuspension in Suisun Bay and SSC in the main channel.

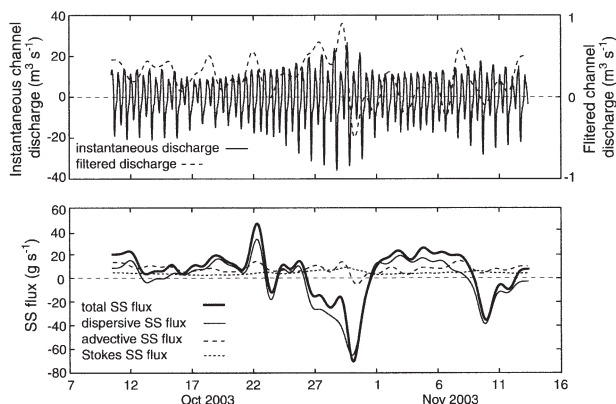


Fig. 12. Instantaneous and filtered channel discharges and suspended sediment (SS) fluxes. Positive values indicate flood direction (towards island interior), negative values indicate ebb direction (towards Suisun Bay).

99% of the total residual suspended sediment flux (Fig. 12). While net advective and Stokes flux were in the landward direction, net dispersive flux was in the seaward direction. During spring tides, dispersive flux was strongly seaward, due to the ebb-dominant tidal currents. Dispersive flux was landward during neap tides, when ebb-dominance ceases. Advective flux again followed the water flux variation. Net sediment flux to Browns Island was in the landward direction, with a magnitude of 14,000 kg during the 34-d deployment (Fig. 13).

The residual sediment flux was affected by the same forcings as the water flux (i.e., tides, wind, barometric pressure). Ebb-dominant flow during spring tides decreased landward flux, while a lack of ebb dominance during neap tides increased landward flux. Friedrichs and Perry (2001) identify ebb-dominant systems as net exporters of sediment; the channels at Browns Island revert from ebb dominance during spring tides to neutral dominance during neap tides, with a corresponding reversal of net transport direction. The net direction of the flux is consistent with previous work in wetlands. As low-energy, fringing areas, wetlands are expected to import sediment and resist erosive processes. Though the marsh proper is erosion-resistant, the channel bed and sides are susceptible to erosion due to high tidal velocities.

We expect that the water imbalance may cause a large sediment imbalance if the unmeasured flow components (groundwater seepage, overland flow, and minor creek flow) are able to transport high concentrations of suspended sediment. Groundwater flow is clearly not a major exporter of sediment. Overland flow would not be able to move large amounts of sediment between the drainage area edge and the creek, due to particle settling and distance. Settling velocities in the Sacramento River

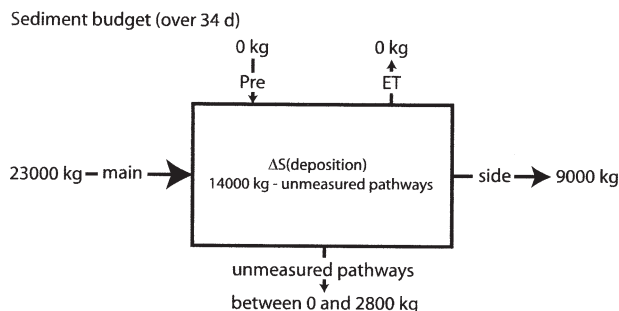


Fig. 13. Sediment budget for Browns Island. Total flux values over monitoring period are given. Suspended sediment concentrations in evapotranspiration (ET), precipitation (Pre), and unaccounted pathways are assumed to be negligible.

were estimated to be between 0.01 and 0.10 mm s^{-1} (Ganju and Schoellhamer 2003); this would require 1.4–14 h to settle in 0.50 m of water. Considering the short period of inundation (approximately 2 h) and low velocities, overland flow should not be able to carry sediment in significant amounts. A parcel of water transiting between the creek edge and the drainage area edge would need to travel approximately 500 m in the 2 h inundation time. This would lead to a water velocity of 7 cm s^{-1} , which is unrealistically high for a salt marsh canopy (Christiansen et al. 2000). Unmeasured creeks may be able to transport at least a mean concentration similar to that of the low-energy side channel (8 mg l^{-1}). Assuming that the remaining water imbalance ($0.12 \text{ m}^3 \text{ s}^{-1}$) is due to unmeasured creeks exporting water, the additional sediment flux over 34 d would be $2,800 \text{ kg}$ (exported). This value is 20% of the net measured import of $14,000 \text{ kg}$.

The measured net import of $14,000 \text{ kg}$ results in an accretion rate of 0.22 mm yr^{-1} , assuming a bulk density of 500 kg m^{-3} and depositional area of 1.3 km^2 . Using a corrected import of $11,200 \text{ kg}$ (considering flux bias), the accretion rate is 0.18 mm yr^{-1} . This analysis ignores the tendency of suspended sediment to deposit near the channel edge (which reduces the area and increases accretion rate), and also assumes all imported sediment deposits on the marsh surface and not the channel bed. Previous research (Reed 2002) suggested higher yearly deposition rates at Browns Island ($>10 \text{ mm yr}^{-1}$), with accumulation maximized between March and August, 1998. Our study occurred during the early fall of 2003 when riverine sediment supply was minimized; 1998 was an extremely wet year with sizeable freshwater flow throughout the summer. Reed's (2002) measurements also cover several seasons and flow regimes.

ERROR ANALYSIS

The error involved in the sediment flux calculation is dependent on measurement limitations and instrument accuracy. The largest single source of error is the lack of a complete water balance, which is to be expected in a porous system. The net water budget shows a net input of $0.20 \text{ m}^3 \text{ s}^{-1}$, which is not measured in output. This may easily be due to groundwater seepage, overland flow, or flow through unmeasured fissures and minor channels. The escape of water through overland flow and groundwater may carry little to no suspended sediment, so flow through unmeasured channels may be assumed to be the major source of any sediment flux bias (2,800 kg export; 20% of net import).

Each component of the aforementioned flux measurement is subject to errors. These errors may be operator-related or simply limitations of the instrumentation. In the following section we decompose each measurement and estimate the associated error. Values are reported for the main and side channel.

Index Velocity Measurement

The mean error of the V_i measurement is 0.26% and 0.68% for the main and side channels, respectively, for all individual 15-min measurements. Individual sample error is a function of sample cell size, averaging interval, and sampling rate (Sontek 2001). Sample cells began 0.20 m from the transducer of the ADCP, while the cells ended at the water surface. This yielded a mean cell size of 4.0 m for the duration of the deployment. The averaging interval used was 360 s for every 900-s measurement interval (15 min), with sampling performed at 20 Hz. The mean error was determined as the average of the individual sample error (0.0002 m s^{-1}) divided by each instantaneous velocity magnitude during the entire deployment.

Channel Average Velocity Measurement

There are three sources of error present in the V_{ca} measurement: the estimation of unmeasured areas of the channel, random errors, and systematic errors (Simpson and Bland 2000). The error involved with the estimation of unmeasured areas is 0.44% for both channels. The estimation of unmeasured areas is necessary due to an inability to measure velocity near the top and bottom of the water column (due to ADCP blanking distance-immersion depth and side-lobe interference, respectively), as well as the edges of the channel. The velocity at the top and bottom of the water profile are estimated by extrapolation using the one-sixth power law, while the edge velocities and depths are

estimated by a ratio-interpolation method that takes channel shape into account. Analysis of more than 100 mid channel profiles yielded a mean measured velocity of 0.3176 m s^{-1} . Fitting a one-sixth power curve to the measured mid channel profile data yielded a mean estimated velocity of 0.3223 m s^{-1} , with an error of 0.0047 m s^{-1} (1.5%). The estimated unmeasured top and bottom discharge in the channel constituted about 30% of the total discharge, so the total error involved in using the power law fit is approximately 0.44%. Due to channel geometry and the use of a small tethered boat, the ADCP was towed extremely close to the channel edges, eliminating the need for large edge estimates. Typical edge discharge estimates were less than 1% of the total discharge, so the error involved with edge estimates is ignored here.

Random error in an individual V_{ca} measurement is estimated at 2.7% of the measured velocity. The random errors associated with the ADCP measurement of instantaneous discharge can be estimated via Simpson and Bland (2000). The relevant variables include the water velocity measurement error, mean water velocity, bottom-track velocity error, error due to natural stream pulsation, depth measurement error, number of ADCP depth bins, number of subsection measurements for one transect, number of water pings per subsection, and the number of bottom pings per subsection. Simpson and Bland (2000) cover the relevance of these variables in detail, as well as the development of the error estimate equation.

Systematic errors, considered negligible here, include instrumental errors, cross-sectional geometry changes, bottom sediment movement, speed of sound changes (due to temperature stratification), and extrapolation of the vertical profile of velocity (Simpson and Bland 2000). Instrumental errors were minimized by following established guidelines for instrument calibration and check-up and field operation. Changes in cross-sectional geometry were assumed to be minimal, as the measurements were made during a single tidal cycle, in a mud-bottom channel. Bottom sediment movement was not present, as suggested by moving bottom checks performed during maximum velocities. Temperature stratification, which alters the speed of sound through the water column, reached a maximum of 0.50°C during the measurement period. This changes the speed of sound (and depth measurement) by 0.13%, which is a negligible error.

Stage Area Relationship

The overall error contribution of the stage area relationship is 2.0%. ADCP depth and bottom-tracking errors are present in the continuous stage record and the channel geometry measurement,

respectively. The accuracy of the upward-looking ADV's pressure sensor is 0.10% (Sontek 2001), while the depth accuracy of the downward-looking ADCP is 2.0% (RD Instruments 2003). Bottom tracking is used to estimate the distance traveled across the channel; errors in this measurement may overestimate or underestimate the width of the channel. The heading sensor error is 2 degrees out of 360, therefore, 0.56%. The bottom track velocity has an error of 0.20% of the total distance (RD Instruments 2003; Hippe personal communication). The total error was determined as the square root of the sum of the individual errors squared.

Index Velocity Rating Curve

Calibrating V_i to V_{ca} produces an average error of 5.5% of the predicted value. The rating curves (Fig. 3) yield predicted values of V_{ca} ; these were subtracted from the measured values and the result was divided by the measured value to provide a prediction error. Values extremely close to slack tide were eliminated due to near-zero velocities but large error. The values for the remaining measurements were averaged to yield the error.

Suspended Sediment Concentration Measurement

The largest single source of error is the estimation of channel-average SSC, which has three components: error in the SSC measurement of water samples, error in the calibration curves, and error of the EDI measurement method (in representing actual channel-average conditions).

The laboratory error of water sample SSC measurement is 14% of the measured value, based on the American Society for Testing Materials method for sediment concentration measurement (ASTM 2002). For the filtration method, errors of 2 and 5.1 mg l⁻¹ are listed for suspensions of 10 and 100 mg l⁻¹, respectively. This dependence of error on concentration was assumed to be linear between 10 and 100 mg l⁻¹, and applied to each sample collected in this study. Errors were computed and averaged to yield the aforementioned value.

The calibration of NTU to channel-average SSC has an error of 22%. The calibration curves (Fig. 8) yield predicted values of channel-average SSC; these were subtracted from the measured values and the result was divided by the measured value to provide a prediction error. The values for all samples in an individual calibration were averaged to yield the error.

The error inherent in the EDI method is 11%. EDI sampling involves representing the entire cross section with five discharge-weighted centroids. Because of lateral and vertical variations, the EDI method cannot precisely measure the channel-

average concentrations. Determining this error is difficult because the actual channel-average value, itself, cannot be measured. A surrogate for SSC can be used to estimate the error. Acoustic backscatter (ABS) measurements are a natural by-product of discharge measurements, and are dependent on the concentration of scattering particles in the water. The measurements made for the V_i calibration contained vertical and lateral profiles of ABS over the entire channel (165 total measurements). These values were corrected for spreading and attenuation losses (Gartner and Cheng 2001). The EDI method was mimicked by calculating the velocity-weighted ABS at the five discharge centroids. The actual channel-average ABS value was taken as the velocity-weighted ABS over the entire channel. The weighted ABS values were converted to SSC values using the time series of channel-average SSC from the turbidity calibration, following the method of Gartner and Cheng (2001). The SSC-ABS calibration was poor at slack tides; flux is negligible at slack, so those points were treated as outliers. The percent difference between the channel-average values and the centroid values was assumed to represent the EDI error. The EDI error using ABS only (without conversion to SSC) was only 2.0%; we have used the conservative value of 11% because ABS is not necessarily an ideal surrogate for SSC.

Total Error Estimate

Using the above values, the total error involved in the net flux measurement is 27% for suspended sediment. This revises the flux estimates as 14,000 ± 3,800 kg for suspended sediment (during 34 d). Considering the bias in water (and sediment) flux would reduce the flux estimate to 11,200 ± 3,000 kg. Assuming that all errors are random and uncorrelated, the total error was estimated as the square root of the sum of the squares of the individual errors. The largest single source of error is the determination of channel-average constituent concentration.

Conclusions

The method described herein is capable of estimating constituent fluxes to and from a tidal wetland, though errors can be significant. Applying these methods at Browns Island produced several major conclusions regarding water and sediment flux. Assuming water storage is occurring within the marsh due to absorption by the peat matrix, changes in water storage are of greater magnitude than residual channel flow. Balancing water input, output, and storage in a porous marsh system is difficult because it is conceptually impossible to measure all transport pathways. This is true even for

a marsh with a well-defined channel system, due to overland flow, subsequent infiltration, and flows through minor fissures and creeks. The net imbalance is 22% of main channel flow. As wind and barometric pressure modulate regional estuarine water levels, marsh water storage also changes. This is one factor determining water and sediment flux on and off the island. Tidal channel erosion is evident during the strongest tides, and advection of suspended sediment is evident in smaller channels within the marsh complex. Wind-wave resuspension in the surrounding estuary increases regional SSC and SSC within the marsh channels. Tidal channel flood-ebb dominance and sediment transport direction vary with the spring-neap cycle. Periods of sediment export and import are determined by this dominance. Due to an unbalanced water budget of 22%, the sediment balance is biased by as much as 20%, due to unmeasured sediment transport through minor water transport pathways, mainly creeks and fissures. Aside from bias due to unmeasured water transport, the largest source of error is the determination of SSC. This includes the use of a surrogate measurement (i.e., turbidity) and the laboratory measurement of water sample SSC. The total error of these flux measurements is 27%.

Sediment flux measurements provide insight on marsh sedimentation processes on finer time scales than surface accumulation studies. Studies show large spatial and temporal variability of surface accumulation throughout a marsh complex, and this confounds analysis of net transport patterns. The net sedimentation for the marsh as a whole is available through sediment flux measurements in major water transport pathways.

Long-term (>1 yr) determination of marsh sediment import requires monitoring over varying meteorological regimes. River flow, wind, barometric pressure, and ambient SSC are highly variable in many estuarine systems. These forcings affect sediment fluxes to and from the wetland on seasonal time scales. In light of sea-level rise and altered sediment delivery from the watershed, the viability of marsh restoration is also dependent on these mechanisms.

ACKNOWLEDGMENTS

This study was supported by the CALFED Bay/Delta Program. The Interagency Ecological Program supported collection of meteorological data in Suisun Bay. Megan Lionberger oversaw all data collection at Browns Island, while Greg Brewster, Paul Buchanan, Brian Downing, Brad Sullivan, and Gail Wheeler provided assistance. Denise Reed is acknowledged for her suggestions regarding the manuscript. Harry Jenter and Victor Levesque are acknowledged for their reviews, and the comments of the anonymous reviewers greatly improved the quality of the manuscript and analysis. Any use of trade, product, or firm names is for descriptive purposes only and does not imply endorsement by the U.S. Government

LITERATURE CITED

- AMERICAN SOCIETY FOR TESTING AND MATERIALS (ASTM). 2002. Standard Test Methods for Determining Sediment Concentration in Water Samples. American Society for Testing and Materials International, ASTM D 3977-97, 11.02. West Conshohocken, Pennsylvania.
- BARTHOLDY, J., C. CHRISTIANSEN, AND H. KUNZENDORF. 2004. Long term variations in backbarrier salt marsh deposition on the Skallingen peninsula—the Danish Wadden Sea. *Marine Geology* 203:1–21.
- CAHOON, D. R., J. C. LYNCH, AND A. N. POWELL. 1996. Marsh vertical accretion in a southern California estuary, U.S.A. *Estuarine Coastal and Shelf Science* 43:19–32.
- CHRISTIANSEN, T., P. L. WIBERG, AND T. G. MILLIGAN. 2000. Flow and sediment transport on a tidal salt marsh surface. *Estuarine Coastal and Shelf Science* 50:315–331.
- EDWARDS, T. K. AND G. D. GLYSSON. 1999. Field methods for measurement of fluvial sediment, p. 1–89. In *Techniques of Water-Resources Investigations*, Book 3. U.S. Geological Survey, Reston, Virginia.
- FISCHER, H. B., E. G. LIST, R. C. Y. KOH, J. IMBERGER, AND N. H. BROOKS. 1979. *Mixing in Inland and Coastal Waters*, 1st edition. Academic Press, San Diego, California.
- FRIEDRICH, C. T. AND J. E. PERRY. 2001. Tidal salt marsh morphodynamics: A synthesis. *Journal of Coastal Research* 27: 7–37.
- GANJU, N. K. AND D. H. SCHOELLHAMER. 2003. Tidal and vertical variability of flocc characteristics, p. 6. In J. P.-Y. Maa, D. H. Schoellhamer, and L. P. Sanford (eds.), *Proceedings of the 7th International Conference on Nearshore and Estuarine Cohesive Sediment Transport Processes*. Virginia Institute of Marine Science Gloucester Point, Virginia.
- GARTNER, J. W. AND R. T. CHENG. 2001. The promises and pitfalls of estimating total suspended solids based on backscatter intensity from acoustic Doppler current profilers, p. 119–126. In G. D. Glysson (ed.), *Proceedings of the 7th Federal Interagency Sedimentation Conference*, U.S. Subcommittee on Sedimentation, Reno, Nevada.
- GOODBRED, S. L. AND A. C. HINE. 1995. Coastal storm deposition: Salt-marsh response to a severe extratropical storm, March 1993, west-central Florida. *Geology* 23:679–682.
- HEMOND, H. F. AND J. L. FIFIELD. 1982. Subsurface flow in salt marsh peat: A model and field study. *Limnology and Oceanography* 27:126–136.
- HEMOND, H. F., W. K. NUTTLE, R. W. BURKE, AND K. D. STOLZENBACH. 1984. Surface infiltration in salt marshes: Theory, measurement, and biogeochemical implications. *Water Resources Research* 20:591–600.
- KRONE, R. B. 1979. Sedimentation in the San Francisco Bay system, p. 85–96. In T. J. Conomos (ed.), *San Francisco Bay: The Urbanized Estuary*. Pacific Division of the American Association for the Advancement of Science, San Francisco, California.
- LEONARD, L. A. 1997. Controls of sediment transport and deposition in an incised mainland marsh basin, southeastern North Carolina. *Wetlands* 17:263–274.
- MARVIN-DIPASQUALE, M. AND J. L. AGEE. 2003. Microbial mercury cycling in sediments of the San Francisco Bay-Delta. *Estuaries* 26:1517–1528.
- NUTTLE, W. K. 1988. The extent of lateral water movement in the sediments of a New England salt marsh. *Water Resources Research* 24:2077–2085.
- NYMAN, J. A., C. R. CROZIER, AND R. D. DELAUNE. 1995. Roles and patterns of hurricane sedimentation in an estuarine marsh landscape. *Estuarine Coastal and Shelf Science* 40:665–679.
- PILLAY, S., L. R. GARDNER, AND B. KJERFVE. 1992. The effect of cross-sectional velocity and concentration variations on suspended sediment transport rates in tidal creeks. *Estuarine Coastal and Shelf Science* 35:331–345.

- PONT, D., J. W. DAY, P. HENSEL, E. FRANQUET, F. TORRE, P. RIOUAL, C. IBANEZ, AND E. COULET. 2002. Response scenarios for the deltaic plain of the Rhone in the face of an acceleration in the rate of sea-level rise with special attention to *Salicornia*-type environments. *Estuaries* 25:337–358.
- REED, D. J. 2002. Understanding tidal marsh sedimentation in the Sacramento-San Joaquin Delta, California. *Journal of Coastal Research* 36:605–611.
- RUHL, C. A. AND D. H. SCHOELLHAMER. 2004. Spatial and temporal variability of suspended-sediment concentrations in a shallow estuarine environment. *San Francisco Estuary and Watershed Science* 2:Article 1. <http://repositories.cdlib.org/jmie/sfews/vol2/iss2/art1>
- SIMPSON, M. R. AND R. BLAND. Methods for accurate estimation of net discharge in a tidal channel. *Institute of Electrical and Electronics Engineers Journal of Oceanic Engineering* 25:437–445.
- SONTEK. 2001. Principles of Operation, Argonaut-Series Instruments. Technical Documentation, Sontek, San Diego, California.
- SUK, N. S., Q. GUO, AND N. P. PSUTY. 1999. Suspended solids flux between salt marsh and adjacent bay: A long-term continuous measurement. *Estuarine Coastal and Shelf Science* 49:61–81.
- TEMMERMAN, S., G. GOVERS, S. WARTEL, AND P. MEIRE. 2004. Modelling estuarine variations in tidal marsh sedimentation: Response to changing sea level and suspended sediment concentrations. *Marine Geology* 212:1–19.
- TOBIN, A., D. H. SCHOELLHAMER, AND J. R. BURAU. 1995. Suspended-solids flux in Suisun Bay, California, p. 1511–1515. *In* W. H. Espey, JR. and P. G. Combs (eds.), Proceedings of the First International Conference on Water Resources Engineering, American Society of Civil Engineers, New York.
- WALTERS, R. A. AND J. W. GARTNER. 1985. Sub-tidal sea level and current variations in the northern reach of San Francisco Bay. *Estuarine Coastal and Shelf Science* 21:17–32.
- WRIGHT, S. A. AND D. H. SCHOELLHAMER. 2004. Trends in the sediment yield of the Sacramento River, California, 1957–2001. *San Francisco Estuary and Watershed Science* 2:2 <http://repositories.cdlib.org/jmie/sfews/vol2/iss2/art2>.
- YANG, S. L. 1998. The role of *Scirpus* marsh in attenuation of hydrodynamics and retention of fine sediment in the Yangtze Estuary. *Estuarine Coastal and Shelf Science* 47:227–233.

SOURCES OF UNPUBLISHED MATERIALS

- CALIFORNIA DEPARTMENT OF WATER RESOURCES. 2002. unpublished data. California Data Exchange Center. <http://cdec.water.ca.gov>.
- HIPPE, R. personal communication. RD Instruments, 9855 Businesspark Avenue, San Diego, California 92131.
- RD INSTRUMENTS. 2003. Workhorse Monitor ADCP specification sheet. <http://www.rdinstruments.com/pdfs/Mon213.pdf>.

Received, June 11, 2004

Revised, August 3, 2005

Accepted, August 26, 2005